Computational Materials Science 252 (2025) 113816

Contents lists available at ScienceDirect

Computational Materials Science

journal homepage: www.elsevier.com/locate/commatsci

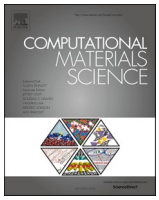

Full Length Article

Layered double hydroxides reinforced epoxy composites: Computational analysis of microstructure effect on strength

Sigitas Kilikevičius [a,*], Leon Mishnaevsky Jr. [b], Daiva Zeleniakiene [c]

[a] Department of Transport Engineering, Kaunas University of Technology, Studentų St. 56, 51424 Kaunas, Lithuania
[b] Department of Wind Energy, Technical University of Denmark, Roskilde 2000, Denmark
[c] Department of Mechanical Engineering, Kaunas University of Technology, Studentų st. 56, Kaunas 51424, Lithuania

ARTICLE INFO

Keywords:
Layered double hydroxides
Epoxy
Composites
Numerical modelling
Mechanical properties
Damage

ABSTRACT

This paper analyses the mechanical and damage behaviour of epoxy composites incorporating magnesium–aluminium layered double hydroxides (LDH), which have potential applications as corrosion protective coatings. The analysis of these composites was carried out by developing a computational model based on numerical homogenisation approach, employing the micromechanical finite element method. The influence of the elastic modulus, aspect ratio and weight fractions of the LDH particles on the mechanical and damage behaviour of epoxy/LDH composites was investigated. Damage modelling was performed, capturing both crack formation and evolution. Damage mechanisms such as crack pinning and crack deflection due to the LDH particles were observed. The modelling demonstrated that with an increase in the weight fraction of LDH, the composite became stiffer and more brittle. Adding up to 5 wt% LDH particles to epoxy increased the elastic modulus of the composite by nearly 20%. The strain at break was reduced to 2 %. The model was validated against experimental data, demonstrating its ability to predict the behaviour of epoxy/LDH composites. The findings indicate that epoxy/LDH composites exhibit enhanced stiffness, making them suitable for practical applications as corrosion-protective coatings.

1. Introduction

Corrosion can be defined as a destructive attack on a material that is caused by reactions with the surrounding environment [1,2]. This phenomenon causes an impairment in the mechanical properties of structures. Various properties such as strength, ductility, or impact strength are affected by corrosion resulting in material degradation. In extreme cases, corrosion leads to ultimate failures of structures [1].

There are several methods to protect structures from corrosion, and one of the most widely used is the employment of protective coatings [3,4]. Coatings serve as a barrier between the material and corrosive environment, thus the penetration of corrosive agent to the material surface can be significantly slowed. Organic coating methods based on epoxy resins have been gaining attention due to their eco-friendliness, low cost, effectiveness, and ease of application [5–7]. Corrosion protection of epoxy-based coatings can be improved by adding anticorrosion pigments [8,9], various nanoparticles [10,11], or corrosion inhibitors [12–14].

Various materials have been developed and researched for use as corrosion inhibitors in protective coatings. Among these, layered double hydroxides (LDH) have emerged as a promising option for corrosion protection. LDH materials are known for their unique structure, which allows them to act as ion-exchangers, making them highly effective at inhibiting the progression of corrosion [15–18]. Epoxies can serve as matrixes, effectively hosting LDH particles, thereby enhancing the protective properties of the coating by providing a synergistic barrier against corrosion [19].

Another important factor is the structural integrity of such a coating. If the coating is easily damaged, the protective effect is impaired, and the structure becomes susceptible to environmental factors. Therefore, it is important to assess the mechanical properties and damage behaviour of coatings during their development. Theoretical and experimental methods are applied to investigate materials composed of various constituents. Theoretical methods provide several advantages such as predicting material behaviour under a very wide range of conditions, optimizing design parameters, and reducing the need for expensive experimentation. Analytical and numerical methods can be applied for research on the mechanical properties of composite materials.

* Corresponding author.
E-mail addresses: sigitas.kilikevicius@ktu.lt (S. Kilikevičius), lemi@dtu.dk (L. Mishnaevsky), daiva.zeleniakiene@ktu.lt (D. Zeleniakiene).

https://doi.org/10.1016/j.commatsci.2025.113816
Received 2 December 2024; Received in revised form 24 February 2025; Accepted 26 February 2025
Available online 2 March 2025

Analytical methods include such as the bounds by Hashin and Shtrikman [20], the self-consistent mechanics model by Hill [21], the Mori-Tanaka model [22], etc. However, analytical methods are restricted to certain geometrical shapes of constituents of composite materials, and they are very limited when it comes to capturing detailed microstructural features, nonlinear behaviours, etc. To address these limitations, numerical methods are used. Finite element-based micromechanical modelling has been shown as a very effective instrument for the research and development of materials composed of various constituents. This approach has been extensively used in a wide range of topics, starting with studies on the elastic properties of composite materials [23–27] and extending to more complex nonlinear behaviour research and damage modelling [28–31].

Various methodologies have been used for computational analyses of epoxy-based composites. Two-dimensional damage models based on the finite element method can be applied to study damage propagation in composite laminates [32]. A two-dimensional micromechanical model was proposed to study the nanoparticle debonding and matrix crack propagation of epoxy reinforced with silica nanoparticles [33]. However, some certain parameters, such as the out-of-plane stress distribution, interlaminar shear effects, spatial crack propagation or the influence of the geometrical orientation of the particles, cannot be accurately determined with two-dimensional models. Three-dimensional models, despite their computational time requirements, can provide more valuable insights. A tree-dimensional damage model of epoxy reinforced with graphene-based nanoparticles has shown that the predominance between the brittle matrix cracking and debonding damage mechanisms of the interface is determined by the orientation of the nanoparticles as well as volume fractions, elastic properties of the materials, and the interface properties [34]. In work [35], three-dimensional crack propagation in an epoxy matrix reinforced with MXene nanoparticles was captured by computational models based on the finite element method, which were solved using explicit dynamic solvers. In work [36], the three-dimensional temperature-dependent damage evolution mechanism of carbon fibre reinforced composites. It was demonstrated that the overall damage morphology and the local fibre/matrix damage behaviour can be captured by micromechanical models based on the finite element method. Micromechanical approaches have also been used recently to address the problematics of fatigue crack growth in epoxy-based composites [37]. In general, recent research demonstrated that the incorporation of additives, even in small fractions, significantly influences the mechanical and damage behaviour of such composites.

Previous studies on epoxy/LDH composite coatings were primarily focused on corrosion protection effectiveness and were largely based on experimental techniques [5,7,19]. However, there remains a lack of computational models to further advance the understanding of epoxy/LDH systems, particularly regarding their mechanical and damage behaviour. The objective of this research is to carry out a computational analysis of the mechanical and damage behaviour of epoxy/LDH composites by developing a computational model based on the micromechanical finite element method that would allow initial insights into the mechanical and damage behaviour of such composites. The proposed model uniquely evaluates the influence of the elastic modulus, aspect ratio, and weight fraction of LDH particles on the mechanical and damage behaviour of epoxy/LDH composites, providing valuable insights for advanced coating design.

2. Materials and methods

A computational model of the mechanical and damage behaviour of epoxy/MgAl-LDH composites was developed using ABAQUS finite element analysis software along with Digimat-FE homogenisation software. The model was based on the micromechanical approach implemented through the finite element method in conjunction with damage mechanics.

For this model, a series of three dimensional computational microstructural geometrical entities that are called representative volume elements (RVEs), were created using Digimat-FE. These geometrical entities of RVEs were imported into ABAQUS. Typical models of RVEs are presented in Fig. 1. The size of the RVEs was 5 times larger than the diameter of the particles, as proposed by the Digimat-FE homogenisation software. As research shows [34,38], this size is sufficient to capture the mechanical and damage behaviour of composites.

Fig. 1(a) shows an RVE measuring 25 μm, containing randomly oriented LDH particles constituting 5 wt%, with a diameter of 5 μm and an aspect ratio (*AR,* the diameter-to-thickness ratio) of 50. Fig. 1(b) shows an RVE measuring 25 μm, containing randomly oriented LDH particles constituting 2 wt%, with a diameter of 5 μm and an aspect ratio of 20.

The RVEs were restrained by boundary conditions that simulate an infinite material domain under uniaxial tensile loading along the x-axis direction. The RVEs were meshed using the three-dimensional 4-node linear tetrahedron element (C3D4) type. A minimum size of 0.5 μm was applied for the mesh, resulting in a total number of 1–1.5 million, depending on the RVE's configuration (Fig. 2).

The multilinear hardening model was applied in the model to define the behaviour of epoxy subjected to mechanical loading. The material model for the epoxy matrix was calibrated using the experimental stress–strain curve of an epoxy material with an elastic modulus of $E_m =$ 2.5 GPa, Poisson's ratio $\nu = 0.35$ and a mass density of 1.08 g/cm^3 (Fig. 3). The experimental stress–strain curve of epoxy was inserted into ABAQUS. Due to the complex geometries with randomly distributed particles and the presence of some plasticity in the analysed materials, a continuum damage model that captures progressive damage based on material degradation was considered. It is suitable for studying bulk material behaviour, including particle–matrix interactions and damage mechanisms, and it is not limited to pre-defined paths. The stresses were calculated using the generalized Hooke's law taking into account damage and plastic deformation [39]:

$$\sigma_{ij} = (1-d)C_{ijkl}\left(\varepsilon_{ij} - \varepsilon_{ij}^{pl}\right) = C_{ijkl}\varepsilon_{ij} + \sigma_{ij}^{in}, \tag{1}$$

where σ_{ij}^{in} is the inelastic stress taking into account both the plastic and damage dissipative mechanisms, C_{ijkl} is the fourth order stiffness tensor, d is the damage indicator expressing the stiffness degradation, ε_{ij} is the total strain, and ε_{ij}^{pl} is the plastic strain.

In this study, the damage model was calibrated to match the experimental data for the epoxy material (Fig. 3). A good correlation between the experimental results and the model was observed when the fracture strain was 0.03. The root mean square error between the experimental curve and the model was 0.233 MPa.

Numerous studies have shown that the elastic modulus of Mg-Al LDH

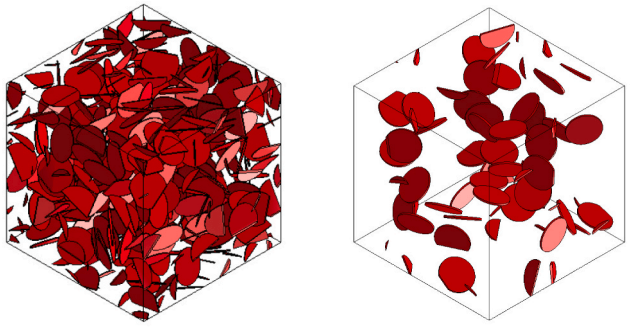

(a) (b)

Fig. 1. Typical models of RVEs: (a) 5 wt%, $AR = 50$; (b) 2 wt%, $AR = 20$.

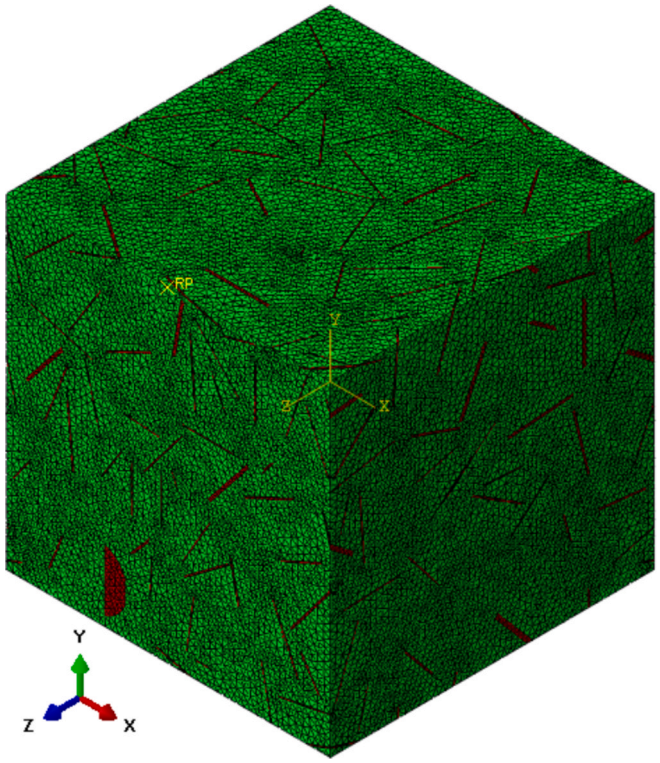

Fig. 2. Finite element mesh of the RVE containing 5 wt% LDH, $AR = 50$.

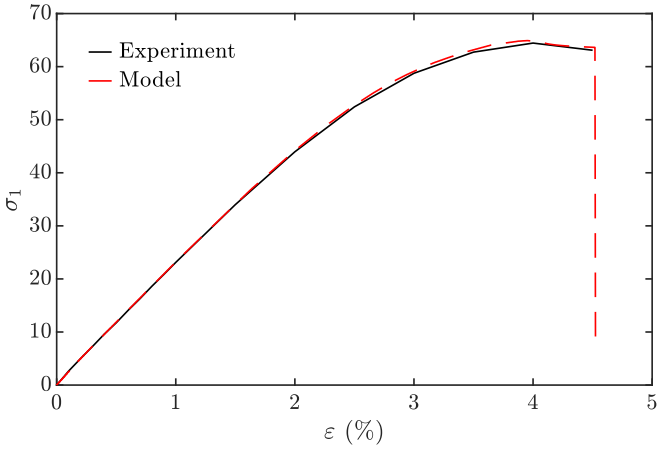

Fig. 3. Calibration of the constitutive material model: comparison of experimental and predicted stress–strain curves for the epoxy material.

typically falls within the range of 1 to 35 GPa [40–42]. On the other hand, molecular dynamics simulations provided a different estimation, indicating that the average in-plane elastic modulus of the entire Mg-Al LDH material was approximately 40 GPa, while a single layer exhibited a much higher modulus of around 135 GPa [43]. Therefore, the elastic modulus of such LDH particles is still the subject of research. Based on the previously mentioned papers, the range between 5 and 20 for the ratio of the elastic modulus of LDH to that of epoxy was investigated in this study on the behaviour of epoxy/Mg-Al LDH composites. The mass density of the LDH particles was set to 1.8 g/cm^3 (as provided by the manufacturer), and Poisson's ratio was set to 0.23, based on the values reported in the literature.

To save computational time, the mass scaling technique was used that modifies the densities of the materials in the model and improves the computational efficiency [44]. The dynamic and inertial effects were not significant as the modelling was carried out as a low kinetic energy process. Moreover, a sensitivity analysis was carried out to evaluate the accuracy of the results. The results at stable time increments greater than $2\bullet10^{-5}$ were very close, while a stable time increment of less than 10^{-4} led to more significant deviations and wavy stress–strain curves. Therefore, the modelling was performed obtaining a stable time increment of at least 10^{-5} s step time.

The developed computational model was solved numerically using the explicit dynamic solver of ABAQUS.

3. Results

Fig. 4 shows the influence of the ratio of the elastic modulus of LDH to that of epoxy on the normalised effective elastic modulus of the composite containing 2 wt% LDH particles. It implies that an increase in the elastic modulus of LDH results in a slight increase in the effective elastic modulus of the epoxy/LDH composite. This trend was slightly more pronounced at the higher aspect ratio.

The obtained results have shown that the addition of LDH particles increases the brittleness of the epoxy/LDH composite. After adding 2 wt % of LDH particles, the strain at break decreased from 4.5 % to approximately 2–2.3 %, depending on the aspect ratio of the particles and the ratio of the elastic modulus of LDH to that of epoxy (Fig. 5). A decrease in the strain at break of the composite was observed with an increase in the ratio of the elastic modulus of LDH to that of epoxy (Fig. 5).

Accordingly, after incorporating 2 wt% of LDH particles, the ultimate tensile stress decreased. This decrease was more significant at a higher aspect ratio. At an aspect ratio of 50, the normalised ultimate tensile stress did not change significantly when the ratio of the elastic modulus of LDH to that of epoxy was between 5 and 20 (Fig. 6). In the same range of the ratio of the elastic modulus of LDH to that of epoxy, the normalised ultimate tensile stress decreased approximately from 0.95 to 0.8 at an aspect ratio of 20.

The stress–strain curves that demonstrate the influence of LDH loading and the aspect ratio on the behaviour of epoxy/LDH composites are presented in Fig. 7. These results showed that with an increase in the weight fraction of LDH, the composite became stiffer and more brittle. This behaviour was more expressed under higher aspect ratios.

This behaviour is reflected by the dependence of the LDH weight fraction on the normalized effective elastic modulus $\overline{E}/E_m$ (Fig. 8). An increase in the elastic modulus was observed with an increase in the weight fraction. With a higher aspect ratio, this trend was more expressed. Adding up to 5 wt% LDH particles to epoxy increased the elastic modulus of the composite by nearly 20 %.

Fig. 9 shows the dependence of the LDH loading on the strain at

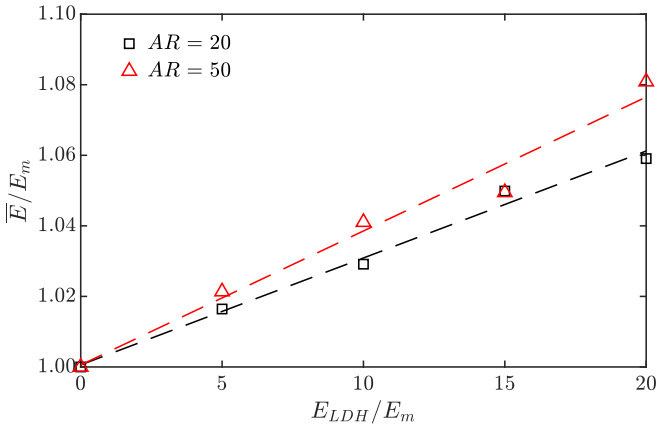

Fig. 4. Normalised effective elastic modulus of the epoxy/LDH composite depending on the ratio of the elastic modulus of LDH to that of epoxy.

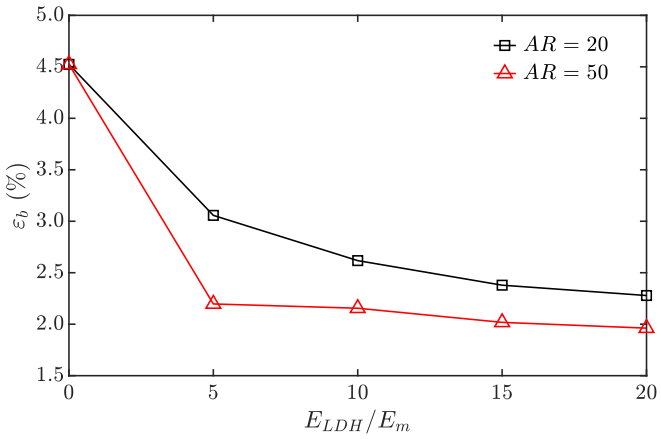

Fig. 5. Influence of the ratio of the elastic modulus of LDH to that of epoxy on the strain at break of the composite.

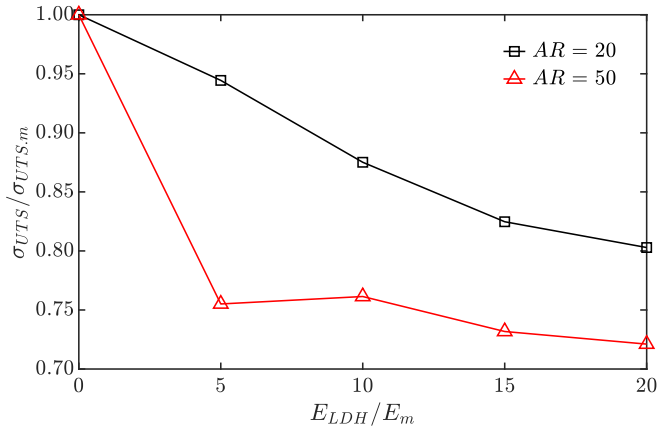

Fig. 6. Influence of the ratio of the elastic modulus of LDH to that of epoxy on the normalised ultimate tensile stress of the composite.

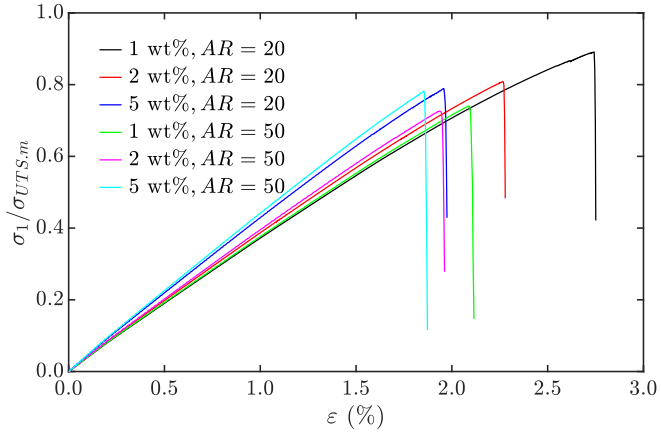

Fig. 7. Normalised stress–strain curves obtained under various weight fractions and aspect ratios of LDH particles, when the ratio of the elastic modulus of LDH to that of epoxy $E_{LDH}/E_m = 20$.

break. If the weight fraction of the particles increases, the composite tends to break at a lower strain. This behaviour was more expressed under a higher aspect ratio. At an aspect ratio of 50, the strain at break decreased from 4.5 % to approximately 2 % after the addition of LDH particles, corresponding to a reduction by approximately 2.25 times. The increased brittleness of the composite could be a limitation in

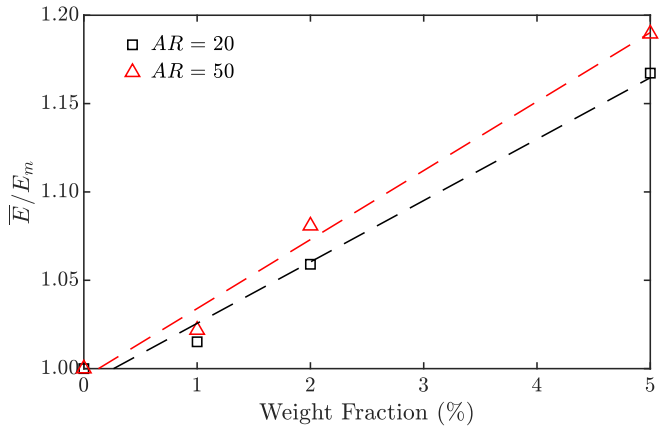

Fig. 8. Normalised effective elastic modulus depending on the LDH loading under different aspect ratios of randomly distributed LDH particles, when the ratio of the elastic modulus of LDH to that of epoxy $E_{LDH}/E_m = 20$.

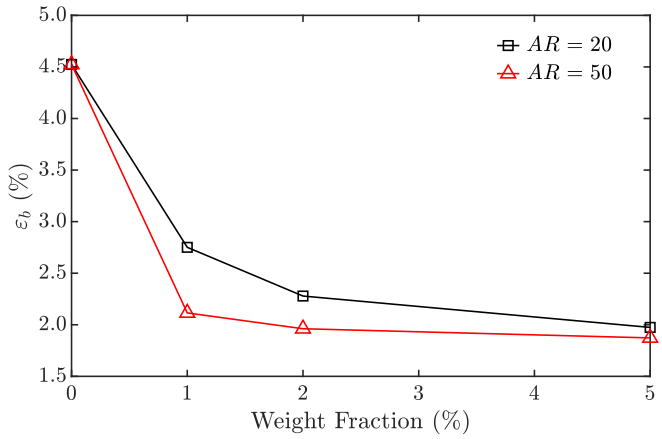

Fig. 9. Strain at break depending on the LDH loading, when the ratio of the elastic modulus of LDH to that of epoxy $E_{LDH}/E_m = 20$.

applications requiring flexibility or those subjected to impacts or other dynamic mechanical loads.

Fig. 10 shows the influence of the LDH loading on the normalised ultimate tensile strength. The tensile strength of the composite was lower than that of pure epoxy. At an aspect ratio of 20, the tensile strength decreased by 10–20 % compared to pure epoxy after adding 1–5 % LDH particles by weight. At a higher aspect ratio, the tensile

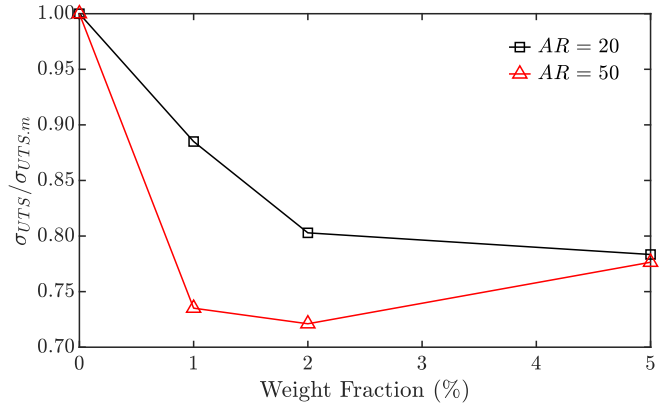

Fig. 10. Normalised ultimate tensile stress depending on the LDH loading, when the ratio of the elastic modulus of LDH to that of epoxy $E_{LDH}/E_m = 20$.

strength decreased by almost 30 % after adding 2 wt% of LDH. A further increase in the LDH weight fraction resulted in a slight increase in the ultimate tensile strength, observed at 5 wt% of the LDH loading. This phenomenon might be caused by improved load transfer efficiency at higher aspect ratios, along with enhanced crack pinning and deflection, leading to localized stress redistribution.

Fig. 11 demonstrates crack evolution at increasing strain levels in an RVE with LDH particles constituting 5 wt%, with an aspect ratio of 50, and the ratio of the elastic modulus of LDH to that of epoxy $E_{LDH}/E_m = 20$. Damage evolution in this RVE is shown in Fig. 12.

Since the LDH particles exhibited significantly higher stiffness and strength, they were not damaged.

Initially, local strain concentrations began to form in the matrix at the edges of the LDH particles (Fig. 11(a)), followed by the formation of cracks in the matrix at the edges of the LDH particles (Fig. 12(a)). The stress and strain concentrations arise due to differences in stiffness between the LDH and the matrix since the LDH particles act as reinforcements. With a further increase in strain, cracks within the matrix structure began to intersect and coalesce, resulting in the formation of the main crack (Fig. 11(b) and Fig. 12(b)). The crack propagated further as the strain increased (Fig. 11(c)-(d) and Fig. 12(c)-(d)).

Damage mechanisms such as crack pinning and crack deflection due to the LDH particles were observed (Fig. 13).

To validate the model, a preliminary experimental study was conducted in accordance with ISO 527 standards. Epoxy/LDH composites were prepared and moulded into dog-bone shaped specimens using silicone moulds. The specimens had a gauge section cross-sectional area of 3 × 1 mm. Tensile tests of developed epoxy/LDH nanocomposites were

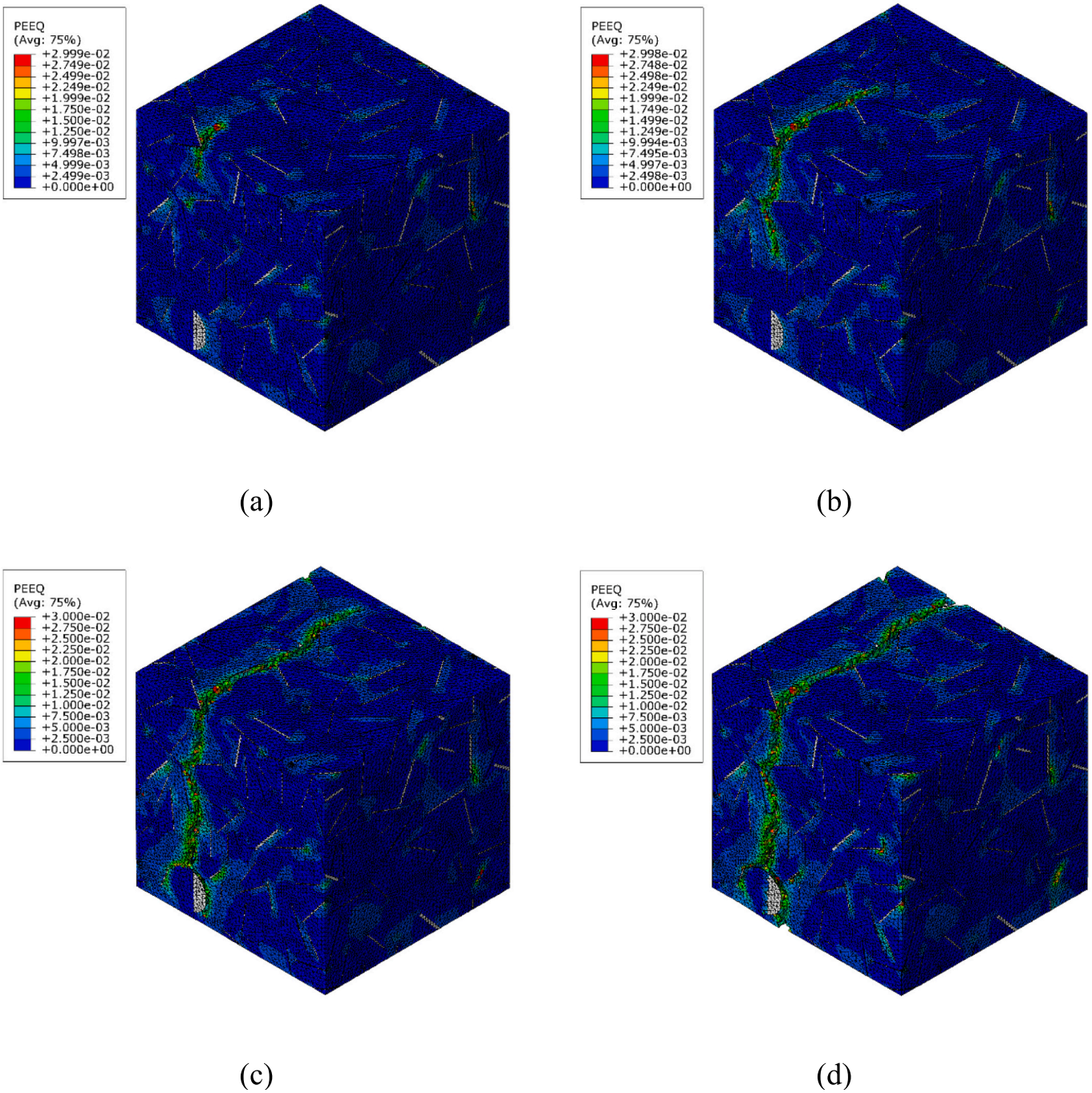

Fig. 11. Equivalent plastic strain contours illustrating crack evolution at increasing strain levels: (a) 1.85%; (b) 1.86 %; (c) 1.87 %; (d) 1.88 %.

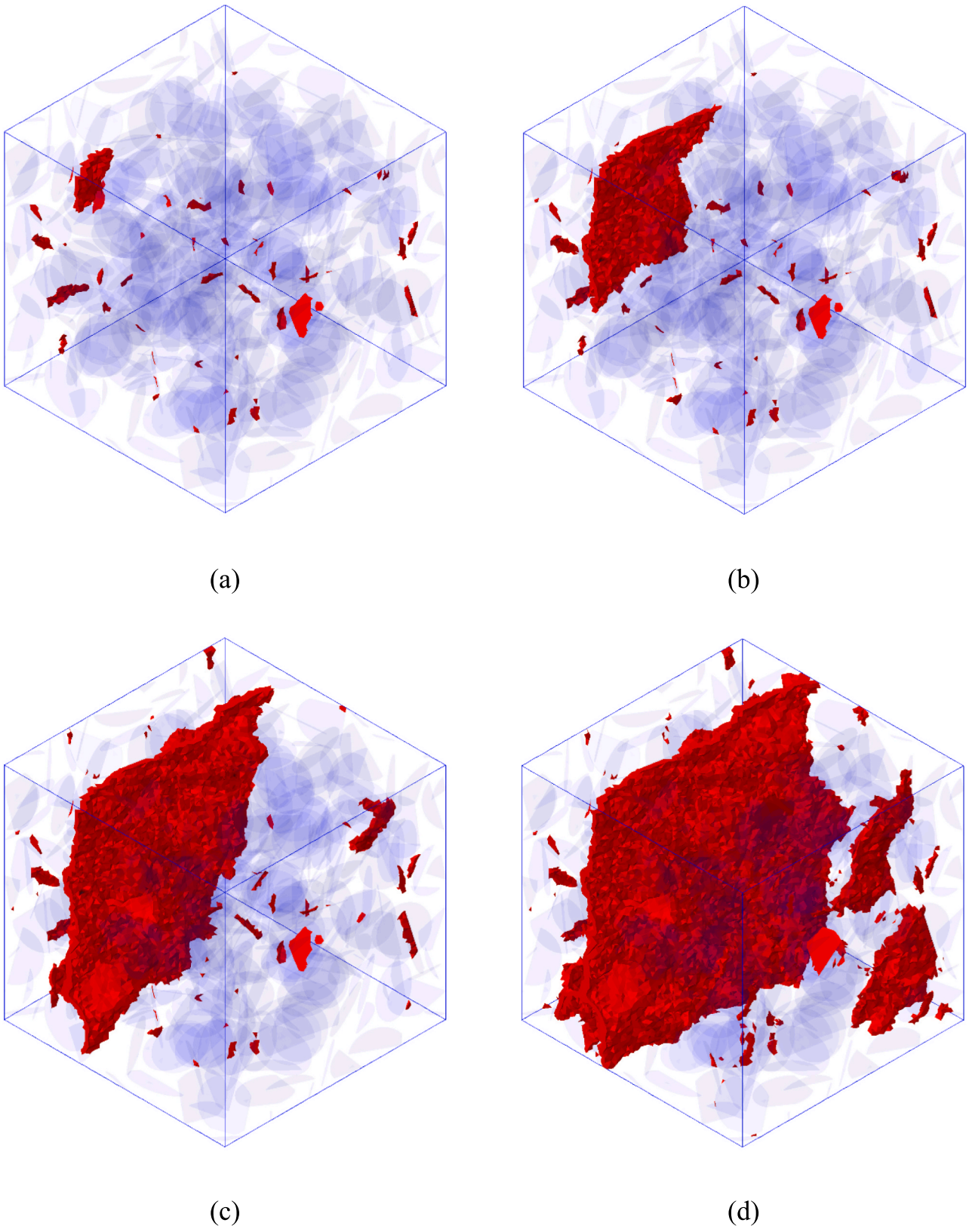

Fig. 12. Damage evolution in the RVE, with damage highlighted in red at increasing strain levels: (a) 1.85 %; (b) 1.86 %; (c) 1.87 %; (d) 1.88 %.

carried out on an *H*10 KT universal column testing machine (Tinius Olsen, Salfords, UK) at a strain rate of 2 mm/min. Five specimens were tested for each fraction. The variability observed in ultimate tensile strength and strain at break is represented by the error bars shown in the experimental results plots (Fig. 14 and Fig. 15).

The experimental data were compared with the model results from a representative volume element (RVE) containing LDH particles with an aspect ratio of 20, and the ratio of the elastic modulus of LDH to that of

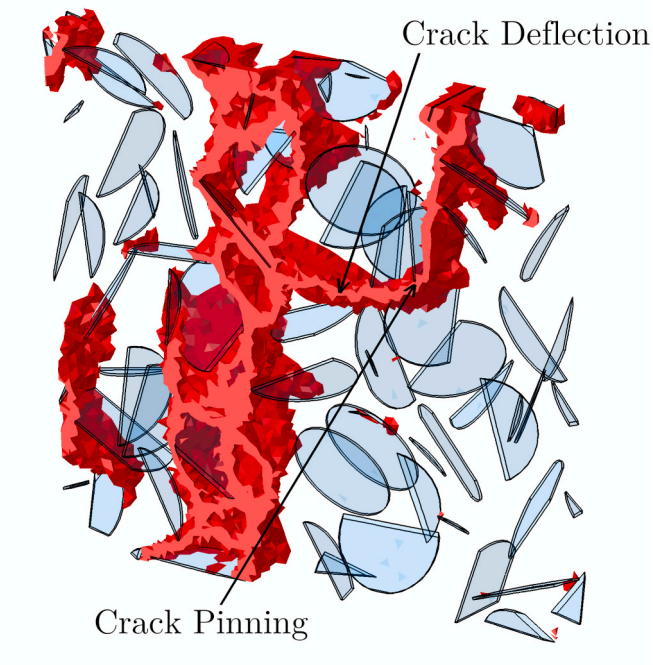

Fig. 13. Crack morphology in the RVE containing 5 wt% LDH, $AR = 50$.

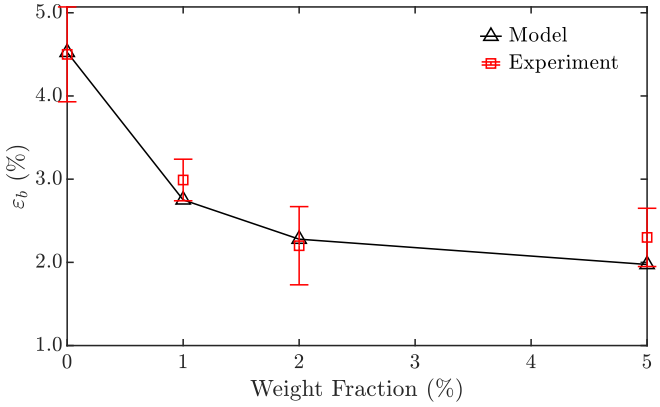

Fig. 14. Strain at break as a function of weight fraction compared with the experimental data.

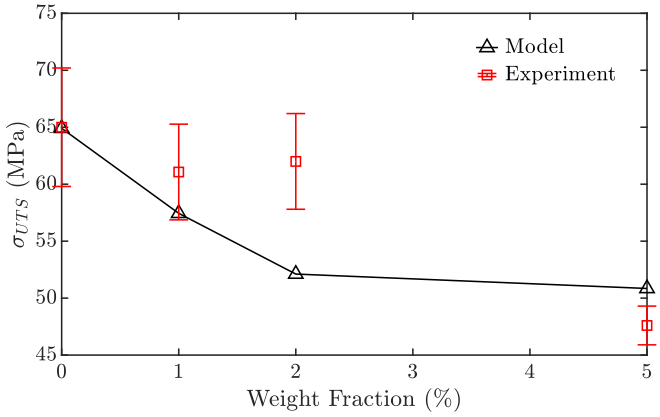

Fig. 15. Ultimate tensile stress as a function of weight fraction compared with the experimental data.

epoxy $E_{LDH}/E_m = 20$. Fig. 14 shows the strain at break predicted by the model compared to the experimental data. A good correlation was observed between the predicted and experimental strain at break of the epoxy/LDH composite.

Fig. 15 shows the ultimate tensile stress as predicted by the model compared to the experimental data. While a similar overall behaviour was captured, notable deviations were observed at certain LDH fractions. The experimental values of the ultimate tensile strength were higher than the model predictions at 1 wt% and 2 wt% LDH, while the opposite was observed at 5 wt%. The discrepancy between experimental and numerical trends can likely be attributed to several factors such as variations in the dispersion of LDH particles within the epoxy matrix during sample preparation, agglomerates, variation in LDH particle sizes, or the perfect particle–matrix bonding of the model.

The presence of agglomerates or clustering of LDH particles could lead to localized stress concentrations, altering the effective reinforcement contribution of the filler and thereby affecting the experimental results. Additionally, variations in LDH particle sizes that are usually present in manufactured composites could introduce inconsistencies in stress transfer, further contributing to deviations from the predicted values. At 5 wt% LDH loading, the experimental tensile strength is lower than predicted. This may be attributed to excessive particle clustering and agglomeration, which can introduce stress concentration sites and weaken the composite structure. The numerical model assumes a uniform dispersion of LDH particles, which could contribute to the differences in the observed strength trends. Furthermore, a higher filler content could negatively impact matrix continuity, reducing load-bearing efficiency and overall strength. Another possible source of deviation is the assumption of perfect particle–matrix bonding in the numerical model. In reality, interfacial adhesion may vary due to processing conditions, leading to imperfect load transfer between the epoxy and LDH particles. This effect is particularly relevant at lower weight fractions, where slight variations in interfacial bonding efficiency can impact mechanical performance. The higher experimental strength observed at lower LDH fractions suggests that LDH particles may act as effective reinforcement due to improved dispersion at lower fractions, leading to changes in stress transfer that are not fully captured in the numerical model. In general, despite the observed deviations, the model provides a reasonable approximation of the experimental results, especially given the inherent complexities of three-dimensional damage modelling in particle-reinforced composites [45,46].

4. Conclusions

A methodology for the modelling of the mechanical and damage behaviour of epoxy/Mg-Al LDH composites has been proposed. It is based on numerical homogenisation approach with the micro-mechanical finite element method.

The influence of the elastic modulus, aspect ratio and weight fractions of the LDH particles on the mechanical and damage behaviour of epoxy/LDH composites was investigated. The modelling demonstrated that with an increase in the weight fraction of LDH, the effective elastic modulus increased and the strain at break decreased, indicating that the composite became stiffer and more brittle. This behaviour was more expressed under a higher aspect ratio. Adding up to 5 wt% LDH particles to epoxy increased the elastic modulus of the composite by nearly 20 %. However, the tensile strength of the composite was lower than that of pure epoxy.

Damage modelling was carried out and the crack formation and evolution was captured. Initially, local plastic strain concentrations at the edges of the LDH particles started to occur, and the formation of cracks was observed locally at the edges of the LDH particles. With a further increase in strain, cracks within the matrix structure began to intersect and coalesce, resulting in the formation of the main crack. As the strain increased, the crack propagated further, eventually leading to final failure. Damage mechanisms such as crack pinning and crack

deflection due to the LDH particles were observed.

The model was validated against experimental data, demonstrating its ability to predict the behaviour of epoxy/LDH composites.

The findings indicate that epoxy/LDH composites exhibit enhanced stiffness, making them suitable for practical applications as corrosion-protective coatings. An increased stiffness suggests that such composites can be advantageous in applications requiring structural rigidity and durability, particularly for static structural components exposed to corrosive environments such as pipelines, storage tanks, marine structures or similar infrastructure components. The increased brittleness of the composite could be a limitation in applications requiring flexibility or those subjected to dynamic loads, such as aerodynamic surfaces or turbine blades.

This study is limited to the mechanical and damage behaviour of the composite under monotonic tension loading. Also, the numerical model assumes a uniform dispersion of LDH particles and perfect particle–matrix bonding. Future work will explore the influence of interfacial bonding effects and agglomeration on the composite's behaviour, as well as its response to cyclic loading. Additionally, it will assess the corrosion protection properties of coatings derived from this composite.

CRediT authorship contribution statement

Sigitas Kilikevičius: Writing – original draft, Visualization, Validation, Software, Methodology, Investigation, Formal analysis, Data curation, Conceptualization. **Leon Mishnaevsky:** Methodology, Software, Writing – review & editing. **Daiva Zeleniakiene:** Writing – review & editing, Supervision, Resources, Methodology, Investigation, Funding acquisition, Formal analysis, Conceptualization.

Funding

The project leading to this application has received funding from the European Union's Horizon 2020 research and innovation programme under the Marie Skłodowska-Curie grant agreement No 101007430.

Declaration of competing interest

The authors declare the following financial interests/personal relationships which may be considered as potential competing interests: [Daiva Zeleniakiene reports financial support was provided by European Commission. If there are other authors, they declare that they have no known competing financial interests or personal relationships that could have appeared to influence the work reported in this paper].

Data availability

Data will be made available on request.

References

[1] J. Bhandari, F. Khan, R. Abbassi, V. Garaniya, R. Ojeda, Modelling of pitting corrosion in marine and offshore steel structures–A technical review, J. Loss Prev. Process Ind. 37 (2015) 39–62, https://doi.org/10.1016/j.jlp.2015.06.008.

[2] R.E. Melchers, R. Jeffrey, The critical involvement of anaerobic bacterial activity in modelling the corrosion behaviour of mild steel in marine environments, Electrochim. Acta 54 (1) (2008) 80–85, https://doi.org/10.1016/j.electacta.2008.02.107.

[3] H. Mirghaderi, R.A. Rahbar, M. Fadavie, The effect of polyurea coating on fatigue life of mild steel, J. of Materi. Eng. and Perform. 30 (5) (2021) 3831–3844, https://doi.org/10.1007/s11665-021-05682-8.

[4] R.A. Yildiz, K. Genel, T. Gulmez, Effect of electroless Ni-B and Ni-WB coatings on the corrosion-fatigue behaviour of 7075 Al alloy, Int. J. Fatigue 144 (2021) 106040, https://doi.org/10.1016/j.ijfatigue.2020.106040.

[5] A. Aminifazl, D.J. Karunarathne, T.D. Golden, Synthesis of silane functionalized LDH-modified nanopowders to improve compatibility and enhance corrosion protection for epoxy coatings, Molecules 29 (4) (2024) 819, https://doi.org/10.3390/molecules29040819.

[6] S. Chhetri, P. Samanta, N.C. Murmu, T. Kuila, Anticorrosion properties of epoxy composite coating reinforced by molybdate-intercalated functionalized layered double hydroxide, J. Compos. Sci. 3 (1) (2019) 11, https://doi.org/10.3390/jcs3010011.

[7] Q. Guo, T. Wang, T.C. Zhang, L. Ouyang, S. Yuan, Superhydrophobic double layered MgAl-LDH/epoxy composite coatings for enhanced anticorrosion performance of magnesium alloys, Prog. Org. Coat. 174 (2023) 107300, https://doi.org/10.1016/j.porgcoat.2022.107300.

[8] M. Fernández- Álvarez, C. Hijón-Montero, A. Bautista, F. Velasco, D. de la Fuente, The effect of additions of anticorrosive pigments on the cathodic delamination and wear resistance of an epoxy powder coating, Prog. Org. Coat. 173 (2022) 107165, https://doi.org/10.1016/j.porgcoat.2022.107165.

[9] I.M. Zin, B.O. DatskoKhlopyk, N.Y. Sobodosh, S.A. Korniy, Effect of zeolite-phosphate anti-corrosion pigment on protective properties of epoxy coating on carbon steel, Mater. Sci., 1–8 (2024), https://doi.org/10.1007/s11003-024-00825-3.

[10] X. Shi, T.A. Nguyen, Z. Suo, Y. Liu, R. Avci, Effect of nanoparticles on the anticorrosion and mechanical properties of epoxy coating, Surf. Coat. Technol. 204 (3) (2009) 237–245, https://doi.org/10.1016/j.surfcoat.2009.06.048.

[11] O.A.A. El-Shamy, M.A. Deyab, Eco-friendly biosynthesis of silver nanoparticles and their improvement of anti-corrosion performance in epoxy coatings, J. Mol. Liq. 376 (2023) 121488, https://doi.org/10.1016/j.molliq.2023.121488.

[12] Y. Jin, H. Duan, S. Zhan, J. Tu, T. Yang, W. Zhang, L. Ma, H. Yu, D. Jia, TiO2 nanocontainers coconstructed using polymers and corrosion inhibitors for anticorrosion reinforcement of waterborne epoxy coatings, ACS Appl. Mater. Interfaces 15 (45) (2023) 52971–52983, https://doi.org/10.1021/acsami.3c12194.

[13] Q. Zhang, M. Shen, X. Liu, H. Fu, W. Yang, J. Zhao, J. Wang, Y. Du, C. Ma, Construction and utilization of rare earth complexes as efficient corrosion inhibitor in epoxy coating, Prog. Org. Coat. 186 (2024) 108024, https://doi.org/10.1016/j.porgcoat.2023.108024.

[14] E. Alibakhshi, E. Ghasemi, M. Mahdavian, B. Ramezanzadeh, A comparative study on corrosion inhibitive effect of nitrate and phosphate intercalated Zn-Al- layered double hydroxides (LDHs) nanocontainers incorporated into a hybrid silane layer and their effect on cathodic delamination of epoxy topcoat, Corros. Sci. 115 (2017) 159–174, https://doi.org/10.1016/j.corsci.2016.12.001.

[15] J. Tedim, T.L. Galvão, K.A. Yasakau, A. Bastos, J.R. Gomes, M.G. Ferreira, Layered double hydroxides for corrosion-related applications—Main developments from 20 years of research at CICECO, Front. Chem. 10 (2022) 1048313, https://doi.org/10.3389/fchem.2022.1048313.

[16] V. Kovalenko, V. Kotok, B. Murashevych, Layered double hydroxides as the unique product of target ionic construction for energy, chemical, foods, cosmetics medicine and ecology applications, Chem. Rec. 24 (2) (2024) e202300260, https://doi.org/10.1002/tcr.202300260.

[17] M.L. Zheludkevich, J. Tedim, M.G.S. Ferreira, "Smart" coatings for active corrosion protection based on multi-functional micro and nanocontainers, Electrochim. Acta 82 (2012) 314–323, https://doi.org/10.1016/j.electacta.2012.04.095.

[18] Y.H.A. Akbari, M. Rostami, M.G. Sari, B. Ramezanzadeh, pH-responsive anti-corrosion activity of gallic acid-intercalated MgAl LDH in acidic, neutral, and alkaline environments, Mater. Today Commun. 40 (2024) 109258, https://doi.org/10.1016/j.mtcomm.2024.109258.

[19] Z. Wang, L. Fang, F. Wu, H. Ruan, Y. Tang, J. Hu, X. Zeng, S. Zhang, H. Luo, Anti-corrosion, self-healing and environmental-friendly Ti3C2Tx/MgAl-LDH@ epoxy composite organic coating for Mg alloy protection, J. Mater. Sci. 58 (7) (2023) 3283–3306, https://doi.org/10.1007/s10853-023-08210-2.

[20] Z. Hashin, S. Shtrikman, A variational approach to the theory of the elastic behaviour of multiphase materials, J. Mech. Phys. Solids 11 (2) (1963) 127–140, https://doi.org/10.1016/0022-5096(63)90060-7.

[21] R. Hill, A self-consistent mechanics of composite materials, J. Mech. Phys. Solids 13 (4) (1965) 213–222, https://doi.org/10.1016/0022-5096(65)90010-4.

[22] T. Mori, K. Tanaka, Average stress in matrix and average elastic energy of materials with misfitting inclusions, Acta Metall. 21 (5) (1973) 571–574, https://doi.org/10.1016/0001-6160(73)90064-3.

[23] A. Alshahrani, S. Kulasegaram, A. Kundu, Elastic modulus of self-compacting fibre reinforced concrete: Experimental approach and multi-scale simulation, Case Stud. Constr. Mater. 18 (2023) e01723, https://doi.org/10.1016/j.cscm.2022.e01723.

[24] R. Sanaka, S.K. Sahu, FEM based RVE modeling for estimating axial modulus of polyurethane composite reinforced with MXene, Int. J. Interact. Des. Manuf. 18 (5) (2024) 3259–3269, https://doi.org/10.1007/s12008-023-01485-4.

[25] S.M. Mirkhalaf, E.H. Eggels, T.J.H. van Beurden, F. Larsson, M. Fagerström, A finite element based orientation averaging method for predicting elastic properties of short fiber reinforced composites, Compos. B Eng. 202 (2020) 108388, https://doi.org/10.1016/j.compositesb.2020.108388.

[26] S.B. Rayhan, M.M. Rahman, Modeling elastic properties of unidirectional composite materials using Ansys Material Designer, Procedia Struct. Integr. 28 (2020) 1892–1900, https://doi.org/10.1016/j.prostr.2020.11.012.

[27] S. Kilikevičius, S. Kvietkaitė, K. Žukienė, M. Omastová, A. Aniskevich, D. Zeleniakienė, Numerical investigation of the mechanical properties of a novel hybrid polymer composite reinforced with graphene and MXene nanosheets 174 (2020) 109497.

[28] A. Pontefisso, L. Mishnaevsky Jr, Nanomorphology of graphene and CNT reinforced polymer and its effect on damage: Micromechanical numerical study, Compos. Part B Eng. 96 (2016) 338–349, https://doi.org/10.1016/j.compositesb.2016.04.006.

[29] H. Ahmadi, M. Hajikazemi, W. Van Paepegem, Predicting the elasto-plastic response of short fiber reinforced composites using a computationally efficient multi-scale framework based on physical matrix properties, Compos. b. Eng. 250 (2023) 110408, https://doi.org/10.1016/j.compositesb.2022.110408.

[30] Y. Chang, Y. Zhou, N. Wang, K. Lu, W. Wen, Y. Xu, Micro-mechanical damage simulation of filament-wound composite with various winding angle under multi-axial loading, Compos. Struct. 313 (2023) 116925, https://doi.org/10.1016/j.compstruct.2023.116925.
[31] J. Jiang, Z. Zhang, J. Fu, H. Wang, C. Ng, A newly proposed damage constitutive model for composite laminates under low-velocity impact by considering through-thickness compression damage, Aerosp. Sci. Technol. 137 (2023) 108267, https://doi.org/10.1016/j.ast.2023.108267.
[32] V. Divse, D. Marla, S.S. Joshi, Finite element analysis of tensile notched strength of composite laminates, Compos. Struct. 255 (2021) 112880, https://doi.org/10.1016/j.compstruct.2020.112880.
[33] Z. Wang, F. Liu, W. Liang, L. Zhou, Nanoscale analysis of tensile properties and fracture of nanoreinforced epoxy polymer using micromechanics, J. Reinf. Plast. Compos. 32 (16) (2013) 1224–1233, https://doi.org/10.1177/0731684413486848.
[34] A. Hussein, B. Kim, Micromechanics based FEM study on the mechanical properties and damage of epoxy reinforced with graphene based nanoplatelets, Compos. Struct. 215 (2019) 266–277, https://doi.org/10.1016/j.compstruct.2019.02.059.
[35] G. Monastyreckis, L. Mishnaevsky Jr, C.B. Hatter, A. Aniskevich, Y. Gogotsi, D. Zeleniakiene, Micromechanical modeling of MXene-polymer composites, Carbon 162 (2020) 402–409, https://doi.org/10.1016/j.carbon.2020.02.070.
[36] T. Zhu, Z. Ren, J. Xu, L. Shen, C. Xiao, C. Zhang, X. Zhou, X. Jian, Damage evolution model and failure mechanism of continuous carbon fiber-reinforced thermoplastic resin matrix composite materials, Composites Sci. Technol. 244 (2023) 110300, https://doi.org/10.1016/j.compscitech.2023.110300.
[37] D. Yang, M. Ma, V. Wei, J. Li, J. Zhou, X. Song, Z. Guan, X. Chen, Multiscale modelling for fatigue crack propagation of notched laminates using the UMAP clustering algorithm, Thin-Walled Struct. 199 (2024) 111819, https://doi.org/10.1016/j.tws.2024.111819.
[38] L. Gao, C. Liu, J. Liu, T. Yang, Effect of subsurface damage on tensile behavior and fracture mechanism of SiCp/Al composites: Experimental analysis and RVE modeling, Eng. Failure Anal. 147 (2023) 107162, https://doi.org/10.1016/j.engfailanal.2023.107162.
[39] Q. Chen, Z. He, Finite-volume micromechanics-based multiscale analysis of composite structural model accounting for elastoplastic and ductile damage mechanisms, Compos. Commun. 45 (2024) 101801, https://doi.org/10.1016/j.coco.2023.101801.
[40] F. Peng, D. Wang, D. Zhang, H. Cao, X. Liu, The prospect of layered double hydroxide as bone implants: A study of mechanical properties, cytocompatibility and antibacterial activity, Appl. Clay. Sci. 165 (2018) 179–187, https://doi.org/10.1016/j.clay.2018.08.020.
[41] J. Labuschagné, D. Molefe, W.W. Focke, O. Ofosu, Layered double hydroxide derivatives as flame retardants for flexible PVC, Macromole. Symp. 384 (1) (2019) 1800148, https://doi.org/10.1002/masy.201800148.
[42] A. Alazreg, M.M. Vuksanović, A. Egelja, I.O. Mladenović, Ž. Radovanović, M. Petrović, A. Marinković, R.J. Heinemann, Mechanical properties of acrylate matrix composite reinforced with manganese-aluminum layered double hydroxide, Polym. Compos. 44 (10) (2023) 6783–6792, https://doi.org/10.1002/pc.27597.
[43] R.L. Anderson, H.C. Greenwell, J.L. Suter, P.V. Coveney, M. Thyveetil, Determining materials properties of natural composites using molecular simulation, J. Mater. Chem. 19 (39) (2009) 7251–7262, https://doi.org/10.1039/b909119j.
[44] D.J. Walters, D.J. Luscher, J.D. Yeager, Considering computational speed vs. accuracy: Choosing appropriate mesoscale RVE boundary conditions, Comput. Methods Appl. Mech. Eng. 374 (2021) 113572, https://doi.org/10.1016/j.cma.2020.113572.
[45] A. Hussein, S. Ramasundaram, B. Kim, A novel method for fabricating bioinspired layered nanocomposites using aligned graphene oxide/PVDF and their micromechanical modeling, Mater. Today Commun. 24 (2020) 101050, https://doi.org/10.1016/j.mtcomm.2020.101050.
[46] N. Despringre, Y. Chemisky, K. Bonnay, F. Meraghni, Micromechanical modeling of damage and load transfer in particulate composites with partially debonded interface, Compos. Struct. 155 (2016) 77–88, https://doi.org/10.1016/j.compstruct.2016.06.075.